

# Model Correlation of Dynamic Non-linear Bearing Behavior in a Generator

Dean Ford, Greg Holbrook, Steve Shields and Kevin Whitacre  
Delphi Automotive Systems, Energy & Chassis Systems

## Abstract

Efforts to correlate the dynamic response of a generator finite element model have revealed a "jump" phenomenon in the experimental vibration measurements of the generator system. The behavior is representative of a non-linear stiffening spring and is believed to be associated with the stiffness characteristics of the rotor shaft bearings. Current modeling techniques provide good correlation between analytical modal analysis results and frequency response functions made with an instrumented impact hammer. However, the resonant frequency of vibration predicted by the generator model does not correlate well with generator response data acquired on an electrodynamic shaker. This paper discusses the non-linear dynamic behavior of the generator response, as indicated by both physical and theoretical data.

## Introduction

Automotive generators are candidates for numerous types of analyses. Computational fluid dynamics is useful in evaluating air flow and fan design. Electromagnetic analyses assist in designing the generator to meet output performance and efficiency requirements. Electrical and mechanical losses generate heat. Static and transient thermal analyses are used to investigate heat dissipation. Structural analysis is applied to achieve durability goals. Often one type of analysis impacts another and requires a coupled field analysis. Structural concerns tend to focus on issues such as modal characteristics, dynamic response, fatigue, stress, strain, or deflection, depending on the situation. These structural concerns often include such non-linear effects as contact, plasticity, and one-sided boundary conditions.

The scope of this paper focuses on the modal characteristics of the generator. Recent attempts to correlate FEA results to the measured generator response in the dynamic realm have proven more contentious than correlation to impact hammer data.

## FEA Model

Historically, for a frequency response function (FRF), the generator structure, as illustrated in Figure 1, has been modeled with the necessary corollary objective to avoid non-linear effects in the model, for size and run-time issues. Globally, the important structural elements of a generator are the frames, fasteners, bearings, and rotor as identified in Figure 2. The stiffness of the rotor is affected by rotor components - such as the shaft, segment, core, and coil. The stator consists of low carbon steel laminations, with soft copper wire windings, and is therefore mainly important for its mass. The finite element model attempts to integrate these important components in a mathematical simulation that accurately represents a nominal design. The most difficult modeling issues tend to be frame to stator interfaces, and modeling bearing stiffness correctly. Each bearing is currently modeled as three mutually orthogonal spring elements as a function of pulley load, which permits appropriate dynamics of the rotor relative to the rest of the generator.

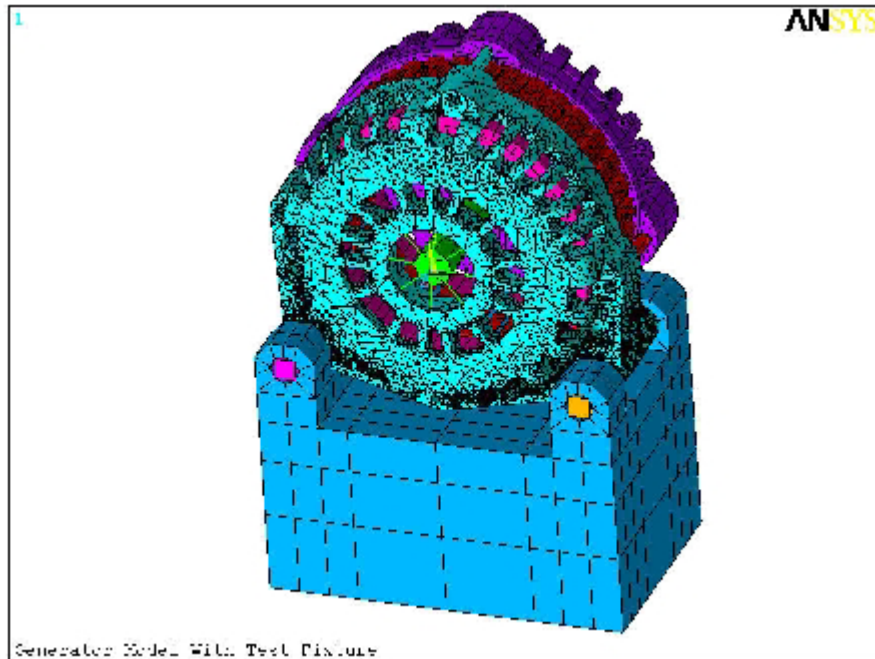


**Figure 1 - Generator Finite Element Model**

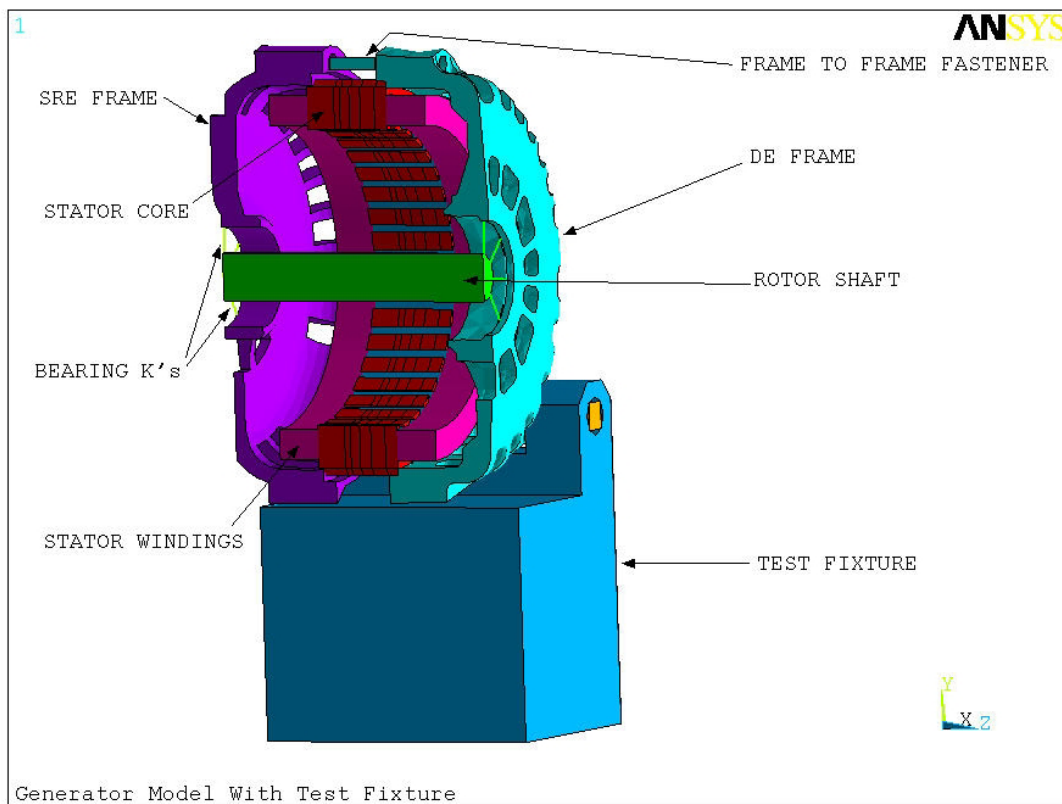


**Figure 2 - Generator Cross Section**

The FEA model in Figure 2 is composed of detailed frame models, a stator, fasteners, a sparse representation of the rotor, bearing stiffness definitions, and the test fixture. The rotor modes occur at high enough frequency that they are not of interest to the authors, thus allowing a sparse representation of the rotor. However, the rigid rotor modes (a function of the stiffness of each bearing) are relevant, as they play a role in many of the lower frequency generator modes. Bearing stiffness is important, as it allows the relevant behavior for these lower frequency generator modes. Other components such as the bridge, regulator, and brush assembly are simply represented as distributed point masses on the back of the rear frame. The resulting model has not incorporated any non-linearity at this point, allowing reasonable solution size and time for dynamic problems. Harmonic response output is limited to a subset of nodes, in order to restrict the problem size. For many cases, excitation is provided as a body load in a given axis, with model restraints attempting to simulate actual physical boundary conditions. Results are often inspected as frequency response functions (output / input), in terms that allow some correlation to physical data.

## Model Correlation / FRF Measurements

Model correlation is conducted by comparing the frequency response functions of a generator finite element analysis (FEA) model and actual parts or subassemblies. The correlating frequency response function is measured from an instrumented impact hammer test. The first step is to correlate general mode shape and frequency information of subassemblies in a free-free state. Next, correlation efforts continue step by step until the FRF of a full generator assembly match within an acceptable tolerance. With a bit of care, correlation of a finite element model to impact hammer testing is achievable within a few percent for the first few modes. One of the main factors affecting correlation is boundary condition simulation. Adjacent structures, such as a mounting bracket, are often included in the finite element model to closer represent the physical test condition. In this case, the vibration test fixture was included in the model.

Figure 3 illustrates the correlation achieved for the first resonant frequency of vibration 160 Hz. This mode could be described as an axial mode of the frames, with the rotor in phase. Note that the amplitudes of the two frequency response functions are in different units, g's acceleration over g's acceleration for the finite element model and g's acceleration over force for the impact hammer. Therefore, the plot is used on a frequency comparison basis only.

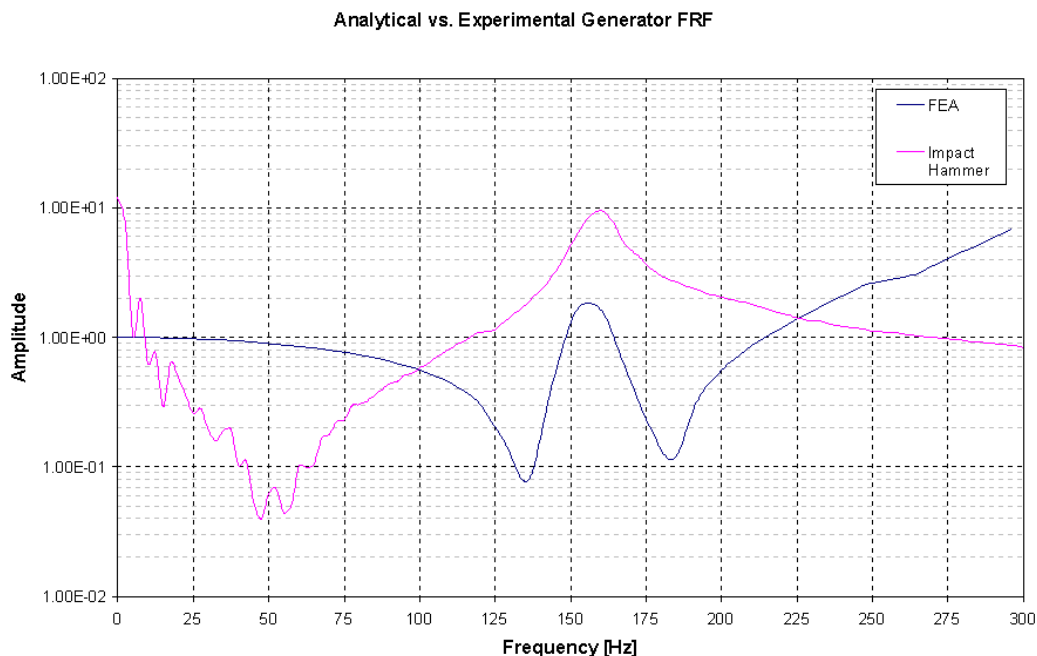


**Figure 3 - Analytical vs. Experimental Generator FRF**

From a test perspective, the relationship between the impact hammer test setup and the vibration durability test conducted on an electrodynamic shaker is also important. It is necessary to properly simulate the dynamic response of the generator in order to develop an accurate vibration durability test. Failure modes may not be reproduced or incorrect failure modes may be created if the generator's dynamic characteristics on the shaker are incorrect. In this case, the impact hammer test incorporated the same vibration test fixture and boundary constraints as in the electrodynamic shaker test. Therefore, it was intriguing to discover a significant difference between the correlated impact hammer model and the shaker resonant frequencies.

## **Electrodynamic Shaker Response Measurements**

A vibration durability test procedure typically includes measuring the generator response using swept sine input. These curves are helpful in identifying the generator/test fixture resonant frequencies of vibration. Figure 4 shows a generator mounted on a vibration test fixture. Although the relationship between the model results and hammer FRF measurements is favorable, the analytical resonant frequency of vibration does not compare well to the generator response data acquired as part of a vibration durability test. The generator response to a 1.0g swept sine excitation is compared to the analytical frequency response function in Figure 5. The figure shows the analytical and experimental data of the first resonant frequency differ by approximately 40 Hz.



**Figure 4 - Electrodynamic Shaker Generator Test Setup**

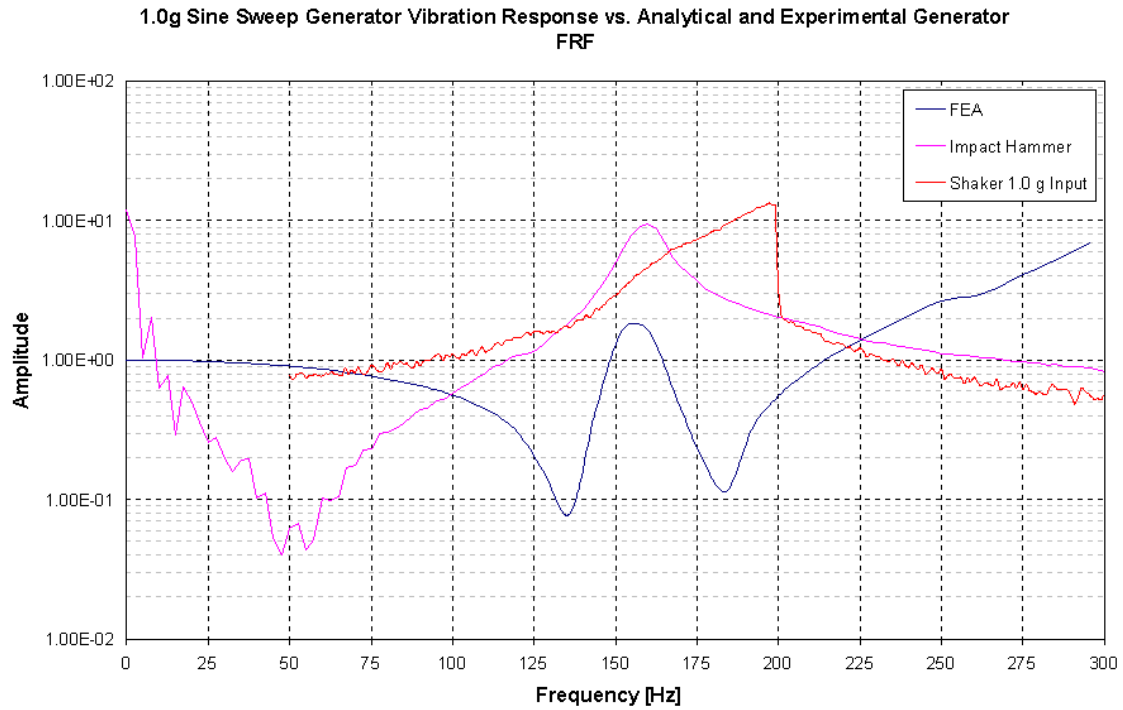


**Figure 5 - 1.0 g Sine Sweep Generator Vibration Response vs. Analytical and Experimental Generator FRF**

To further investigate this discrepancy, a series of tests were conducted using different random input excitation levels. The resonant frequency for a 0.7 Grms flat random input profile matches reasonably well with the hammer FRF and analytical data as shown in Figure 6. However, increasing the excitation level raises the frequency of the resonance. The resonant frequencies for the various excitation levels are plotted in Figure 7. The 200 pound pulley load curve indicates the frequency of the resonance increases nearly 60 Hz over this input range. Figure 7 also shows the effect of pulley load on the resonant frequency. The resonant frequency is approximately the same for an 80 pound and 200 pound pulley load above 4.0 Grms. Below 4.0 Grms, the difference in the resonant frequency for the two pulley loads becomes larger as the input excitation is reduced.

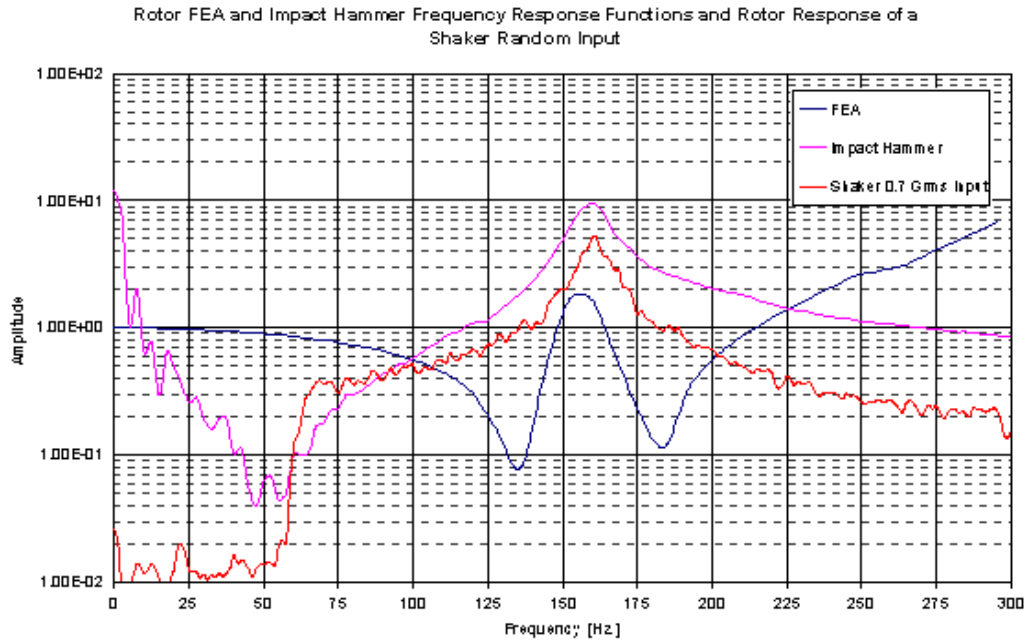


**Figure 6 - 0.7 Grms Random Input Generator Vibration Response vs. Analytical and Experimental Generator FRF**

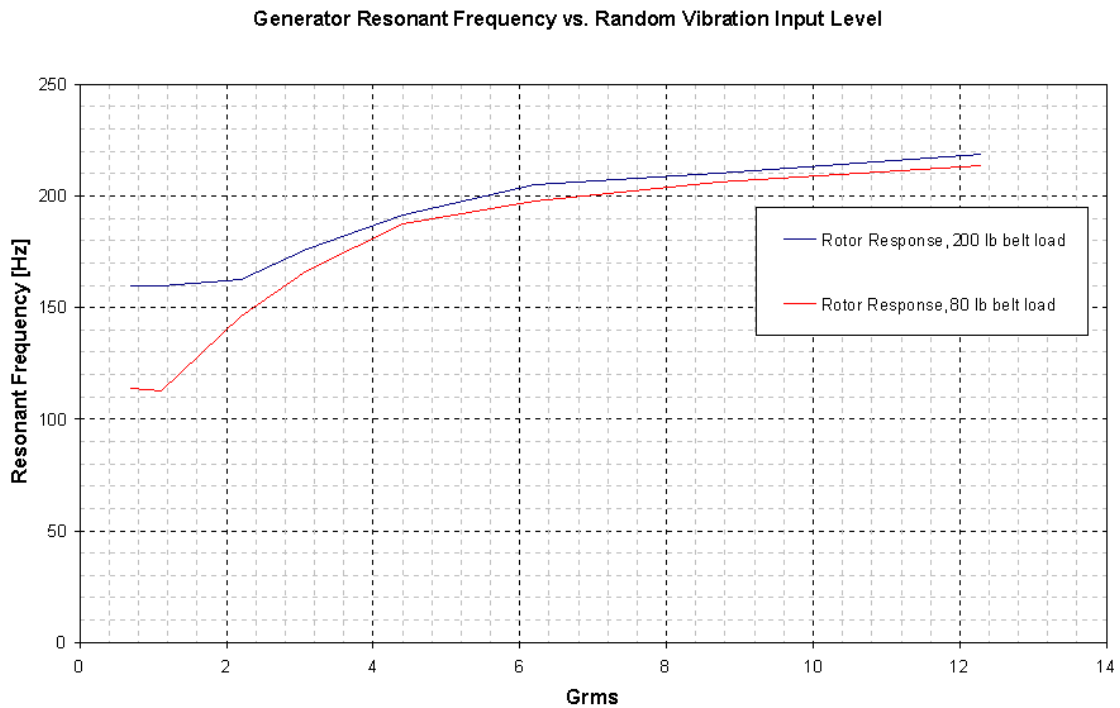


**Figure 7 - Generator Resonant Frequency vs. Random Vibration Input Level**

Pre-loading the rotor shaft bearings in the axial direction with shims between the pulley and drive end housing increases the frequency of the resonance as shown in Figure 8. The greatest impact occurs at the lower input excitation levels where the frequency increases as much as 100 Hz with respect to the non-shimmed case for the 200 pound belt load. Note the frequency of the resonance decreases slightly as the input excitation increases when the bearings are pre-loaded. Also, the change in resonant frequency over the input range is only 20 Hz with the shims installed compared to 60 Hz for the non-shimmed case.

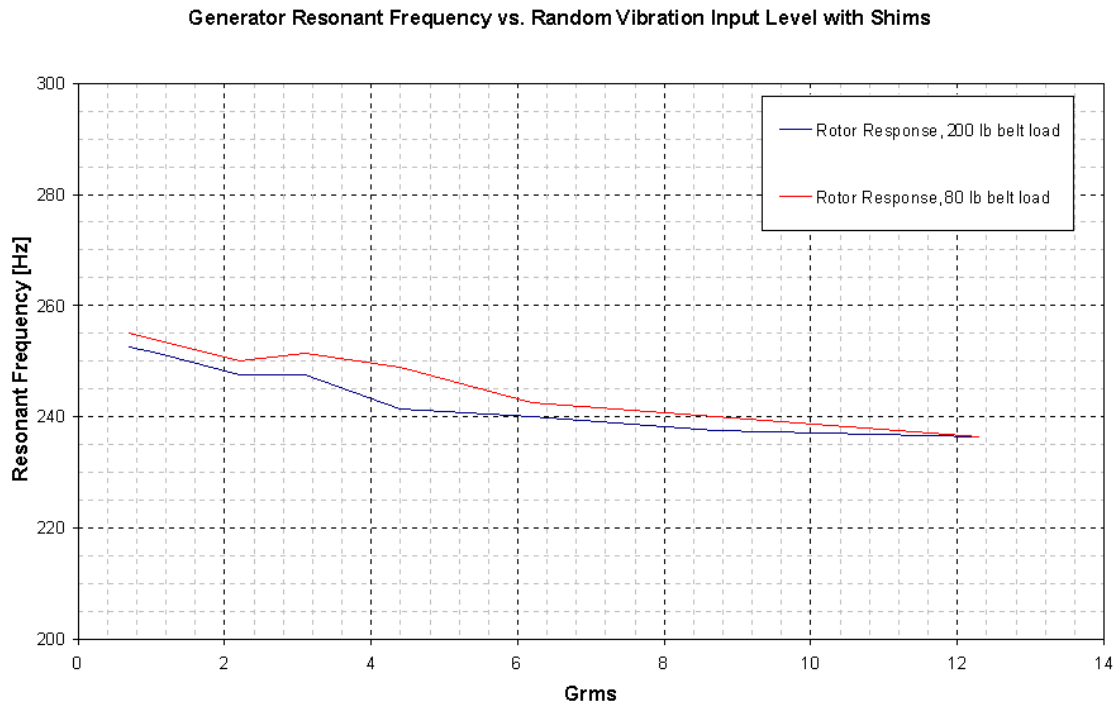


**Figure 8 - Generator Resonant Frequency vs. Random Vibration Input Level with Shims**

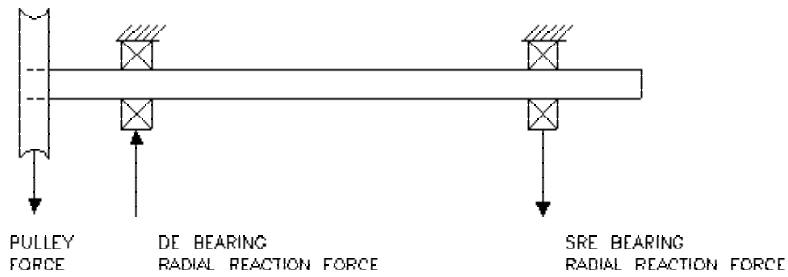
The random vibration input data indicates excitation level, belt tension, and bearing pre-load can significantly affect the resonant frequency. Based on these observations, a major contributor to the difference between the finite element model calculations and the swept sine electrodynamic shaker test results is likely related to the rotor shaft bearings.

## Non-linear Math Model

The non-linearity in the bearing may be treated as a stiffening spring as described by Thomson and Dahleh [1] and Tse, Morse, and Hinkle [2]. If the bearing acts as a stiffening spring, two non-linear phenomena should be observed. First, if the structure is excited with a slowly swept sine, the sweep up in frequency will yield a different response than when swept down in frequency. The second phenomenon is the presence of harmonics in the response function, especially the third harmonic.

The ball bearings support the shaft, rotor, and pulley. There is a lateral pulley load caused by the belt which will result in radial loading on the bearings, even for a static situation as illustrated in Figure 9. Under dynamic and vibration loading, the bearings will support both axial and radial loads, in addition to the nominal belt load reactions.

The non-linearity in the ball bearing can be explained in a simplified manner by examining Figure 10, which shows a single ball in a cross section view. In order to explain the fundamentals, assume that all of the radial load in each bearing is supported by a single ball, which is in compression. (The total picture is more complicated, but the explanation of the non-linearity does not change.)



SHAFT WITH PULLEY AND TWO BALL BEARINGS

**Figure 9 - Rotor / Bearing Load Schematic**

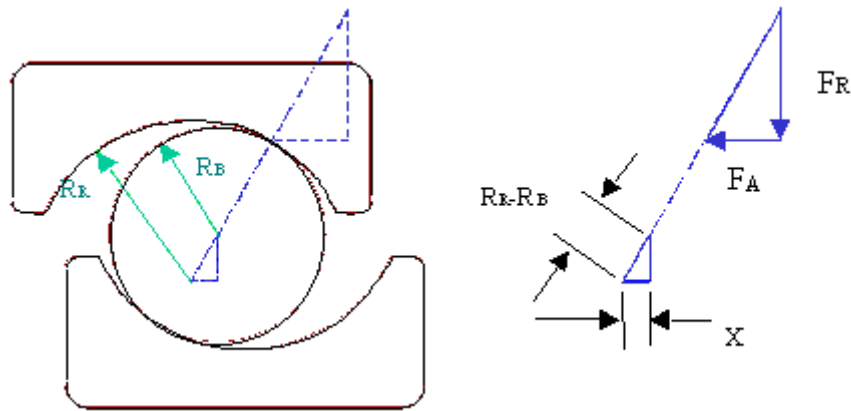


**Figure 10 - View of Axially Displaced Bearing Section**

Examine a single ball of radius  $R_B$ , which is restrained between the circular bearing races with radii of  $R_R$ . If the ball is supporting a given radial load, which is a reaction to the belt force, then as the inner race shifts axially relative to the outer race, an axial force develops. To support the radial load, this axial force must have the magnitude given by the following equation:

$$F_A = F_R \frac{x}{\sqrt{(R_R - R_B)^2 - x^2}} \quad (1)$$

where:

- $R_R$  race radius
- $R_B$  ball radius
- $x$  axial displacement of the race relative to the center of the ball
- $F_R$  radial force, which is imposed by the reaction to the belt load
- $F_A$  resultant axial load resulting from the axial displacement  $x$

Since the total bearing deflection is the summation of the outer and inner race displacements relative to the ball, the force equation written in terms of the total relative race deflections is:

$$F_A = F_R \frac{z}{\sqrt{4 \cdot (R_R - R_B)^2 - z^2}} \quad (2)$$

where  $z$  is the combined axial displacement of the outer race relative to the inner race.

If  $z \ll 4 (R_R - R_B)$ , then the bearing will behave approximately as a linear spring. However, as  $z$  increases the bearing acts as a stiffening spring.

As a first approximation to the non-linearity, the spring can be treated as a linear spring with an added cubic term. If a nonlinear term proportional to  $x^3$  is added to the basic single degree of freedom vibration equation, the following equation results ( $x^3$  is used instead of  $x^2$  so that the compressive and tensile regimes are identical except for their sign).

$$m\ddot{x} + c\dot{x} + kx + \mu \cdot x^3 = A \cdot \sin(\omega t) \quad (3)$$

where:

$x$	displacement
$m$	mass
$c$	damping coefficient
$k$	linear stiffness
$\mu$	coefficient of the cubic term
$A$	amplitude of the driving force
$\omega$	driving frequency (radians per unit time)
$t$	time

To examine this phenomenon in its simplest terms, one can look at the transient response of the single degree of freedom equation with a non-linear stiffening term. If the amplitude of the resulting oscillations is plotted against  $\omega$ , the sweep up and sweep down responses around the resonance will differ from each other. A transient solution of the differential equation results in the plot shown in Figure 11. The red curve is obtained when the frequency is increasing and the blue curve is obtained when the frequency is decreasing. Note the curves exhibit the two phenomena associated with a stiffening spring, as discussed earlier, the resonant frequency is different for the ascending and descending sine sweeps and the third harmonic is present.

Amplitude of Response from Equation 3

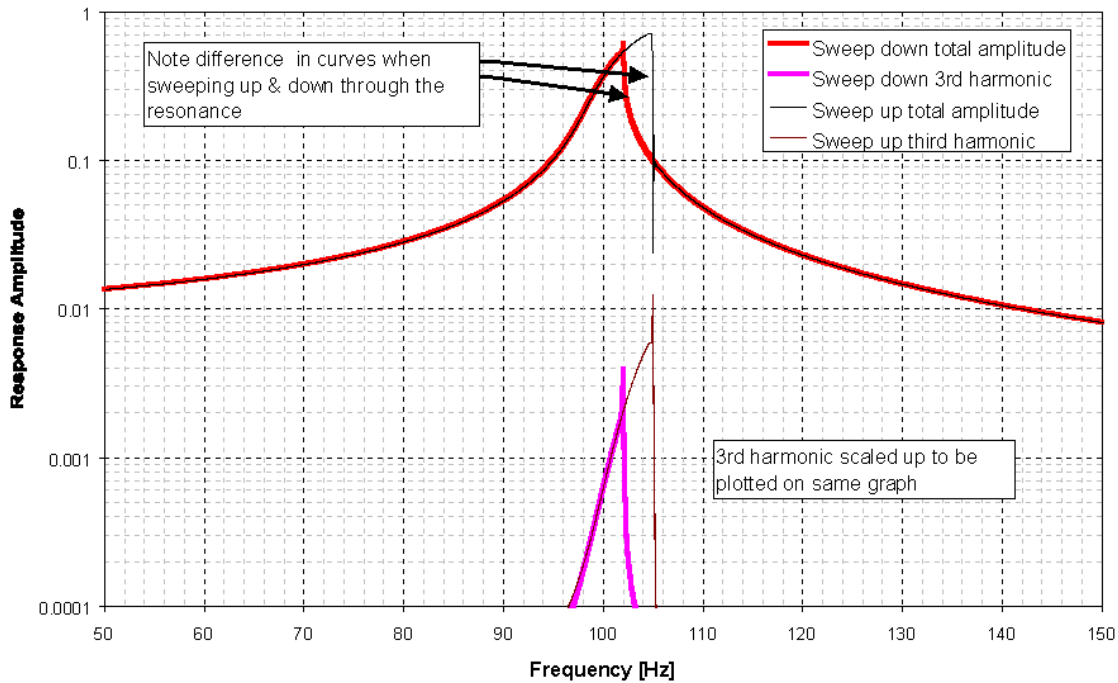


Figure 11 - Non-Linear Response - Sine Sweep Up & Down

Experimental measurements were acquired on an electrodynamic shaker using varying input excitation levels to test this hypothesis. Data was collected while increasing and decreasing the frequency for each level of the sine input. Comparing the ascending and descending sine sweep curves makes it possible to detect the "jump" phenomenon associated with a stiffening spring. At low excitation levels, the resonant frequency is the same for the ascending and descending sine sweep curves. Figure 12 contains the generator vibration response curves for a 0.25g sine input. However, the frequency shift is present in the data for excitation levels 0.5g and higher. In addition, the "jump" phenomenon becomes more pronounced as input levels increase. The frequencies are significantly different for the 3.0g sine input curves as shown in Figure 13. Placing the ascending sine sweeps for the various levels on one plot as found in Figure 14 illustrates the classic non-linear stiffening spring characteristic depicted in textbooks. Waterfall digital signal processing techniques were employed to check for the presence of harmonics in the rotor response data. Waterfall maps were created using the swept sine input as a trigger signal. Data was acquired at approximately 4.0 Hz intervals. Figure 15 contains the rotor response waterfall map for a 1.0g ascending sine sweep. The spectra confirm harmonics of the resonant frequency exist in the rotor response measurements.

0.25g Sine Sweep Generator Vibration Response

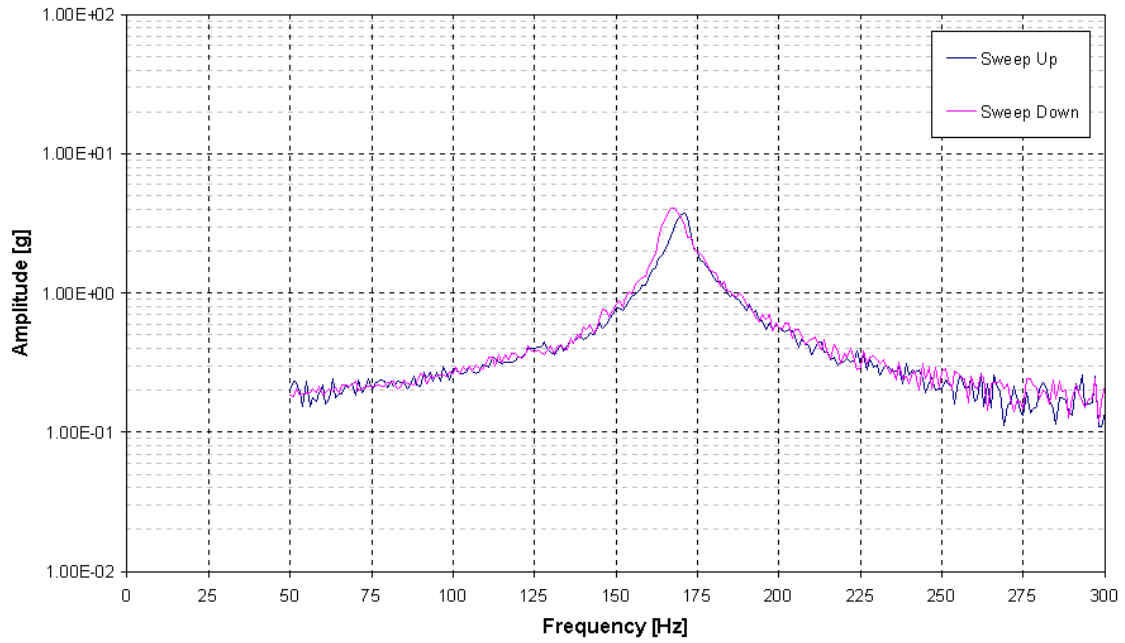


Figure 12 - 0.25 g Sine Sweep - Generator Vibration Response

3.0g Sine Sweep Generator Vibration Response

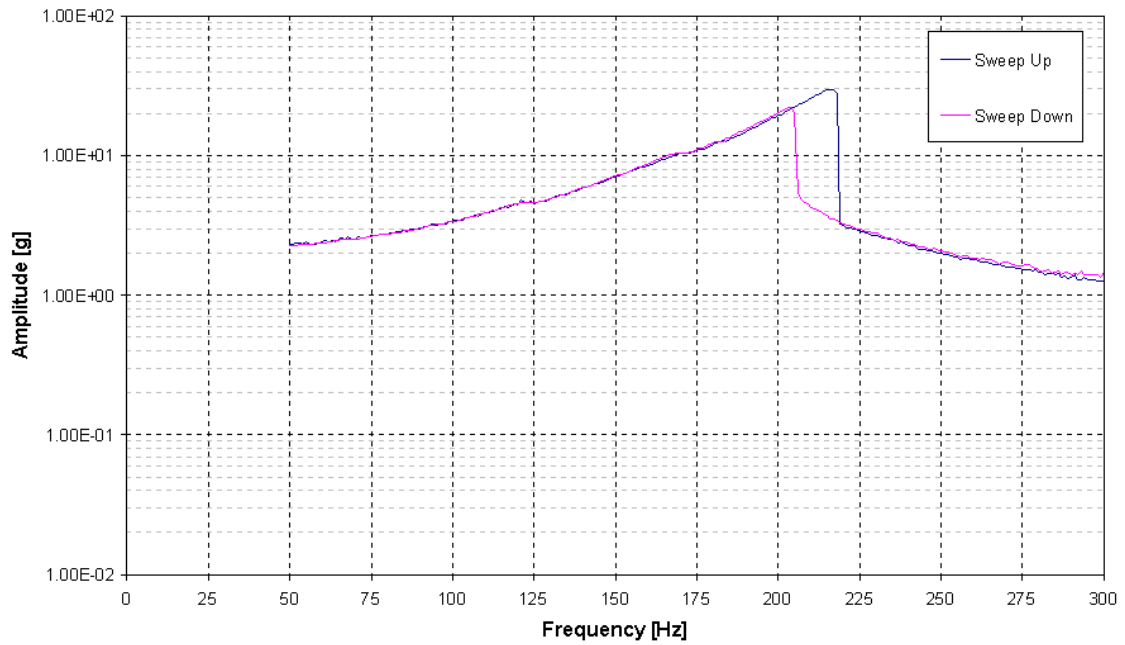


Figure 13 - 3.0 g Sine Sweep - Generator Vibration Response

Ascending Sine Sweeps - Generator Vibration Response

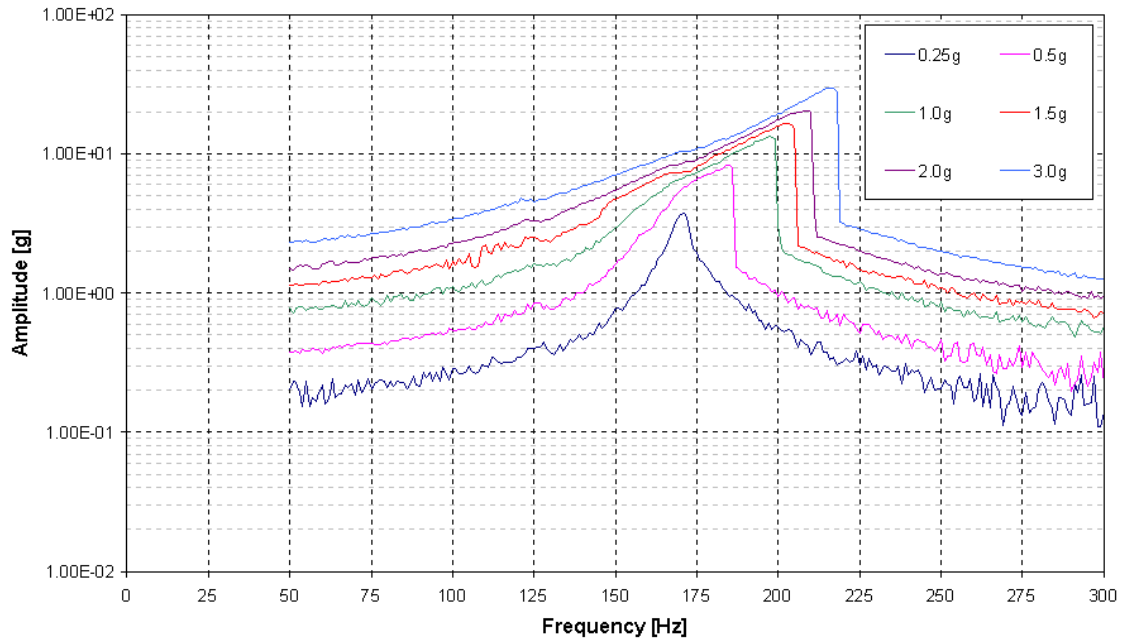


Figure 14 - Ascending Sine Sweeps – Generator Vibration Response

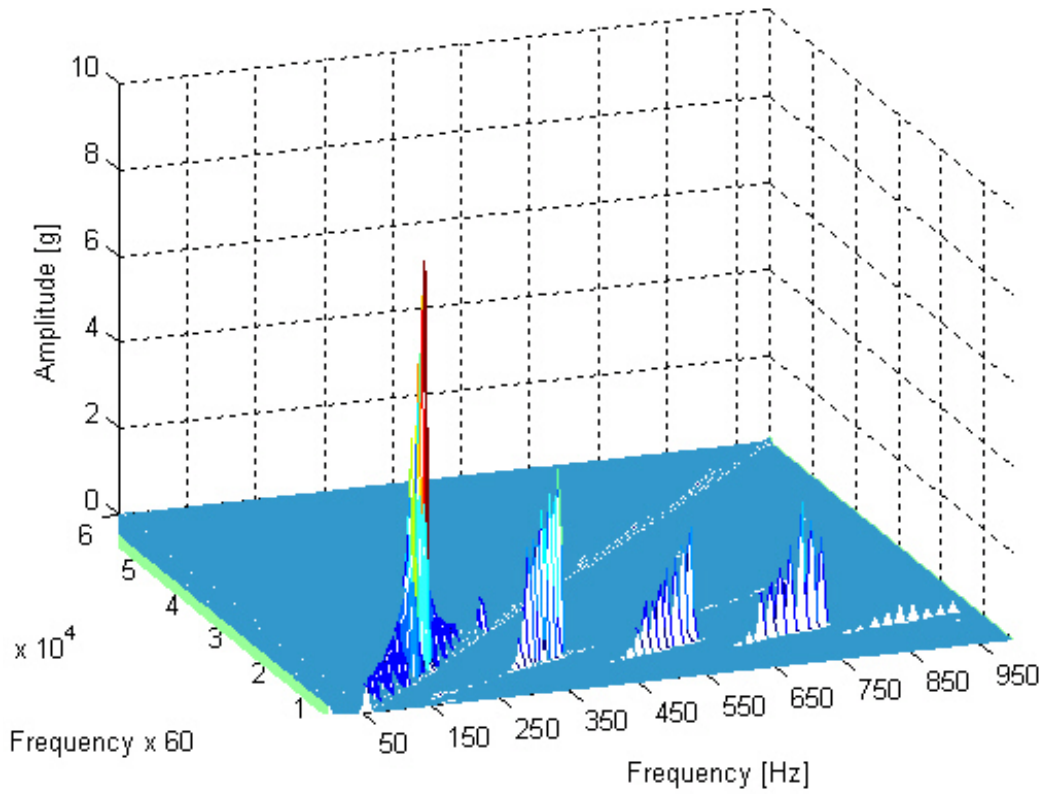


Figure 15 - 1.0 g Sine Sweep Waterfall Map

## Conclusion

Investigating the correlation between finite element model calculations, instrumented impact hammer data, and electrodynamic shaker response measurements has resulted in a better understanding of the rotor shaft bearing characteristics and how they influence the dynamic response of the generator. It is possible to describe the impact of the bearing as a non-linear stiffening spring. Measured generator vibration response curves have shown similar "jump" phenomenon as predicted by the math model of the bearing. Based on this theoretical description for the bearing, the next challenge is to develop methods to accurately model this behavior.

In order to include the nonlinear effect of the bearing in future structural models, the most straightforward method would be to perform a transient dynamic analysis. In order to do this efficiently, it would be necessary to reduce the linear portion of the model to a small model either by dynamic sub-structuring or component mode synthesis (a feature not yet implemented in ANSYS). This would also allow the inclusion of the gyroscopic stiffening effect caused by the spinning rotor. At this time, the authors have not yet attempted this next step.

## References

- [1] W. T. Thomson and M. D. Dahleh; Theory of Vibration With Applications, 5th ed., Prentice Hall Inc., Simon & Shuster - A Viacom Co., 1998, Upper Saddle River, New Jersey
- [2] F. S. Tse, I. E. Morse and R. T. Hinkle; Mechanical Vibrations - Theory & Applications, 2nd ed.; Allyn & Bacon Inc., 1979, Boston, MA.